Eur. Phys. J. A **21**, 257–263 (2004)
DOI 10.1140/epja/i2003-10205-1

THE EUROPEAN PHYSICAL JOURNAL A

Production and decay of the isotope ^{271}Ds (Z = 110)

K. Morita[1,a], K. Morimoto[1], D. Kaji[1,2,b], H. Haba[1], E. Ideguchi[1,b], R. Kanungo[1], K. Katori[1], H. Koura[1,3], H. Kudo[2], T. Ohnishi[1], A. Ozawa[1,c], T. Suda[1], K. Sueki[4], I. Tanihata[1], H. Xu[5], A.V. Yeremin[6], A. Yoneda[1], A. Yoshida[1], Y.-L. Zhao[7], and T. Zheng[8]

[1] RIKEN (The Institute of Physical and Chemical research) Wako-shi, Saitama 351-0198, Japan
[2] Niigata University, Ikarashi, Niigata 950-2181, Japan
[3] Advanced Research Institute for Science and Engineering, Waseda University, Okubo, Shinjuku-ku, Tokyo 169-8555, Japan
[4] University of Tsukuba, Tsukuba, Ibaragi 3058577, Japan
[5] Institute of Modern Physics, Chinese Academy of Science, 730000 Lanzhou, PRC
[6] Flerov Laboratory of Nuclear Reactions, JINR, RU-141 980 Dubna, Russia
[7] Institute of High Energy Physics, Chinese Academy of Science, Beijing 100039, PRC
[8] School of Physics, Peking University, Beijing 100871, PRC

Received: 22 September 2003 / Revised version: 26 December 2002 /
Published online: 10 August 2004 –
Communicated by J. Äystö

Abstract. Production and decay of the isotope ^{271}Ds were studied. The isotope was produced by ^{208}Pb + ^{64}Ni → ^{271}Ds + n reaction. Fourteen α-decay chains have been assigned to decays originating from the isotope ^{271}Ds. An excitation function of the production of this isotope was measured. The results have provided a good confirmation of production and decay of ^{271}Ds reported by Hofmann *et al.* The presence of an isomeric state in ^{271}Ds has been confirmed. The existence of a possible isomeric state in ^{267}Hs is presented.

PACS. 23.60.+e α decay – 25.70.-z Low and intermediate energy heavy-ion reactions – 27.90.+b $220 \leq A$

1 Introduction

To search for heaviest elements is one of the interesting subjects in experimental nuclear physics. New elements whose atomic numbers were greater than 101 were synthesized by heavy-ion–induced fusion reactions. Because the fissility of a heavy system increases with the increase of the atomic number, the production cross-sections of heavy systems tend to decrease exponentially with the increase of the atomic number. The main difficulty in searching of the heaviest elements arises from the small production cross-sections. For example, the cross-section measured for producing ^{277}112 was reported to be 0.5 pb [1]. The small cross-section is limiting further the research of nuclei with greater atomic numbers. To overcome the difficulty more intense primary beams as well as rapid and efficient separation methods that guarantee low rates of background particles (scattered particles or target nuclei, products from reactions other than complete fusion) must be applied. From the beginning of the year 2002 the RILAC (RIKEN Linear ACcelerator) facility started the operation in higher energy (up to 5.8 A MeV) after installation of the additional accelerator CSM (Charge State Multiplier) [2]. The accelerator complex of the RILAC facility (18 GHz ECR ion source [3], RFQ linac [4], original RILAC [5], and the CSM) provides the suitable beam for studying very heavy systems. A gas-filled recoil separator GARIS [6] was installed in the experimental hall of the RILAC facility for studies of heavy elements utilizing the full advantage of the accelerator complex. As a first attempt, we studied the production and decay of ^{271}Ds. The isotope was produced by the ^{208}Pb + ^{64}Ni → ^{271}Ds + n reaction. The present work has confirmed the experimental results obtained at GSI, reported by S. Hofmann *et al.* [7–9].

The excitation function for producing very heavy nuclei by fusion-evaporation reaction provides important information on the reaction mechanism. Systematic studies of optimum reaction energies which give the maximum yield for heavy-element production are also very important to estimate the optimum energy for studying heavy systems. From the experimental point of view, however, the measurement is rather difficult because the production

[a] e-mail: morita@rarfaxp.riken.go.jp
[b] *Present address*: Center for Nuclear Science, University of Tokyo, Wako-shi, Saitama 351-0198, Japan.
[c] *Present address*: University of Tsukuba, Tsukuba, Ibaragi 3058577, Japan.

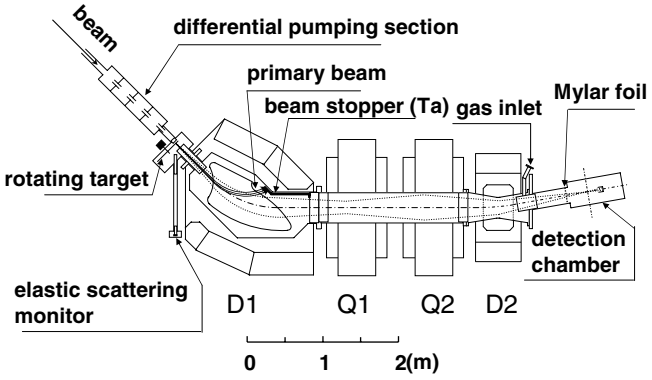

Fig. 1. Plane view of RIKEN GARIS. The shape of dipole magnets is shown in the figure. Envelopes of evaporation residues are shown by dotted lines. The typical trajectory of primary beam is also shown.

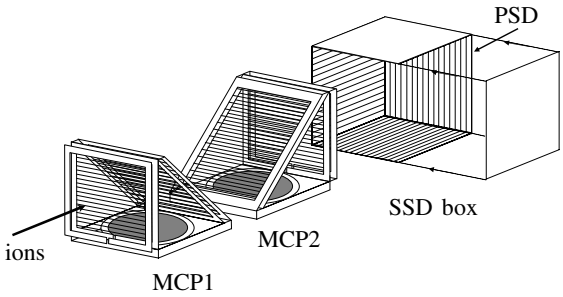

Fig. 2. Schematic drawing of the detection system at the focal plane of GARIS.

cross-sections are very small for producing isotopes of heavy elements having atomic numbers greater than 110. Although a systematic study of the excitation function for heavy-element production via cold-fusion reaction was reported by Hofmann [7], the statistical error of the measured cross-sections for nuclei with $Z > 110$ is large because of the small numbers of decay events obtained in adequate irradiation times. We have measured the excitation function as part of the future plan to produce heavier nuclei.

Synthesis of the isotope ^{271}Ds was confirmed consequently. In heavy-element research, a reproduction experiment done by a different group with a different device to confirm one result is important. As far as element 110 is concerned, productions of ^{269}Ds [10], ^{271}Ds [8], and ^{270}Ds [11] were reported by Hofmann *et al.*, GSI in Germany, and production of ^{273}Ds [12] was reported by Lazarev *et al.*, FLNR of JINR in Russia, and ^{267}Ds [13] by Ghiorso *et al.*, LBNL in USA. But there are almost no experiments to confirm the same nuclide by different groups. Recently, the LBNL group reported the confirmation of ^{271}Ds [14] by observing two decay chains starting from the isotope. The present work provided a concrete confirmation of a production of ^{271}Ds using the same reaction, but a type of experimental device different to that used in the previous experiment [8].

2 Experimental procedure

We used the gas-filled recoil separator GARIS at the RILAC facility. The plane view of the experimental setup is shown in fig. 1. The setup consists of a differential pumping section, a rotating-wheel target, a magnetic recoil separator filled with helium gas, and a detection section.

Ions of ^{64}Ni were accelerated by RILAC. The beam was introduced to the target chamber into the gas-filled region after passing through the differential pumping section. Thus, no foils were needed to separate the vacuum region of the beam transport system from the gas-filled region. Reaction products of our interest recoiling out of the targets were separated by GARIS from the primary beam or unwanted particles such as target recoils or transfer reaction products. Then the products were implanted into the semiconductor detector placed at the focus of GARIS.

Cross-sections were measured at four beam energies. The energy was measured by two methods. One was by measuring the magnetic-rigidity $B\rho$ value using a 90° bending magnet. The other one was a time-of-flight method using two cylinder-shaped electrode sets in the straight section of the beamline. The difference between the energies determined by the two methods was $\sim 0.2\%$. The overall ambiguity in energy determination was ± 0.6 MeV.

The targets were prepared by evaporation of ^{208}Pb metal (isotopically purified up to 98.4%) deposited on carbon backing foils of 30 μg/cm^2 thickness. The thicknesses of the targets ranged from 190 μg/cm^2 to 270 μg/cm^2. An additional 10 μg/cm^2 carbon layer was evaporated on the target to protect the target from sputtering. The beam hit the target from the 30 μg/cm^2 foil side. Eight targets were mounted on the rotating wheel, which rotated by a speed of 1000 rpm. The beam hit the wheel at the distance of 6.25 cm from the pivot.

The beam intensity and the target condition were monitored by measuring elastically scattered beam particles by a PIN photodiode located 45° from the beam axis. The beam intensity was deduced from the counting rate of the elastically scattered particles assuming the scattering is pure Rutherford scattering.

GARIS consists of four magnets in D1-Q1-Q2-D2 configuration where D and Q denote dipole and quadrupole magnets, respectively. The primary beam was stopped in a tantalum plate located inside the chamber of the D1 magnet. The role of the D2 magnet is to reduce the background from light particles otherwise detected in focal-plane detectors. The pressure of the helium gas filled in GARIS was 75 Pa. The $B\rho$ value of GARIS was 2.04 Tm.

The reaction products transported to the focal plane of GARIS were detected by the focal-plane detectors. Schematic view of the detectors is shown in fig. 2. The detection area was separated from the gas-filled area by a 1 μm Mylar foil and evacuated down to 1.3×10^{-4} Pa. The products passed two foils of timing counters shown in fig. 2 as MCP1 and MCP2. Micro channel plates were used for detecting secondary electrons emitted from the

foils. The effective areas of the counters were 78 mm in diameter. A distance between the foils was 29.5 cm. Then the products were implanted into a position-sensitive silicon semiconductor detector (PSD) that has an effective area $60 \times 60\,\mathrm{mm}^2$.

Signals from the timing counters were used for two purposes. One was to obtain information on masses of heavy products using their time-of-flight (TOF) between two foils of the timing counters, and the energy signals from the PSD. The other was to distinguish decay events in the PSD and the implantation events.

The identification of the products was based on genetic correlations of mother and daughter nucleus. All successive decays started from the products after the implantation took place at the same position and in anticoincidence with the timing detectors. We could identify the products by the time, position, and energy correlation of the decay signals.

Because stopping ranges of α-particles were much larger than that of fusion products, α-particles emitted in backward hemisphere escaped from the detector. Four silicon detectors (SSDs) of the same size as the PSD but not position sensitive were set in box shape in backward direction of the PSD in order to detect the α-particles escaping from the PSD.

The energy resolution for decay α-particles measured only by PSD was 70 keV (FWHM), while that for those measured as sum of PSD and SSD was 140 keV (FWHM). These resolutions were improved to 35 keV and 70 keV, respectively, in the November run by cooling the detectors down to 0 °C in temperature.

The beam intensity typically was 5×10^{12} /s and the singles counting rate of the PSD at this beam intensity was 3 to 10 /s. The counting rate depended strongly on the target condition. Main components of the signals were due to the target recoils and the scattered beam particles. The counting rate of the decay signals (no signal in timing counters) was about 1 /s.

The detection system was periodically checked by detecting evaporation residues from the $^{\mathrm{nat}}$Ce + ^{64}Ni reaction. Energy calibration of the PSD and SSD was also done regularly.

3 Experimental results

We performed the experiment in three periods: July, September and November. The date, energy in front of the target, beam dose, number of events corresponding to the decays of ^{271}Ds, average thickness of the targets used, and corresponding cross-sections are summarized in table 1. To deduce the cross-section, the efficiency of GARIS was estimated to be 0.80 ±0.15. The efficiency of GARIS was measured to be 0.8 for ^{208}Pb + ^{58}Fe → ^{265}Hs + n reaction in the preparatory experiment [6]. The listed errors of the cross-sections are only statistical ones with 68% confidence level. T_{av} denotes thickness of the targets deduced from the weighted average used through the irradiation.

The production cross-sections measured in different periods agree well within the statistical errors. Therefore we could combine the results of different periods at the same incident energies to deduce the cross-sections with better counting statistics. The results are summarized in table 2 together with the beam energies at the half-thickness of the targets. The energy widths caused by the energy loss of the projectiles in the targets are also listed in the table. The energy losses were calculated using ref. [15].

Table 1. Summary of the measurement in the year 2002. E_{in}: energy from the accelerator. T_{av}: average target thickness.

Date	Days	E_{in} (MeV)	Dose 10^{18}	Number of events	T_{av} (μg/cm^2)	σ (pb)
12.07–25.07	14	310	1.00	1	230	$1.8^{+4.1}_{-1.5}$
25.07–01.08	8	313	0.59	3	250	$9.0^{+8.1}_{-5.1}$
19.09–22.09	4	313	0.36	1	190	$6.4^{+15}_{-5.3}$
24.09–28.09	5	316	0.88	7	220	16^{+8}_{-6}
28.09–01.10	4	320	0.42	0	210	< 9.0
09.11–11.11	3	320	0.59	0	210	< 6.4
11.11–12.11	2	316	0.19	2	230	19^{+26}_{-13}

Table 2. Summary of the excitation function measurements. E_{in}: primary-beam energy. E_{c}: energy at the half-depth of the target. ΔE: energy loss of the beam in the target. T_{av}: average target thickness.

E_{in} (MeV)	E_{c} (MeV)	ΔE (MeV)	Dose 10^{18}	T_{av} (μg/cm^2)	Number of events	$\sigma^{(\mathrm{a})}$ (pb)
310 ± 1	308	±1.3	1.00	230	1	$1.8^{+4.1}_{-1.5}$
313 ± 1	311	±1.2	0.95	230	4	$8.0^{+6.0}_{-4.0}$
316 ± 1	314	±1.2	1.07	220	9	17^{+7}_{-6}
320 ± 1	318	±1.1	1.01	210	0	< 3.7

($^{\mathrm{a}}$) Errors in the cross-section and upper limit are given in terms of 1σ confidence level.

We totally observed fourteen decay chains attributed to the decays of ^{271}Ds in three experimental periods. Energies and decay times are listed in table 3 by the order of observations. In the energy column, energies marked by **a** indicate energies fully measured by the PSD, while those marked by **b** indicate energies obtained by the sum of the PSD and one of the SSDs. Because of energy losses in the dead layers at the surface of the detectors, the energy resolution measured by the sum of two detectors was much worse than the one measured by only PSD.

Totally 58 α-decays were registered. Thirty-three of 58 decays were in category **a** (57%), and 25 decays were in category **b** (43%). For seven of the fourteen chains (# 1, 2, 5, 6, 7, 8, and 11), 6-fold (ER-α1-α2-α3-α4-α5) correlations were observed, where ER denotes the evaporation residue. For four chains (# 9, 10, 12, and 14), 5-fold correlations were observed. For two chains (# 3, and 13) 4-fold correlations were observed. For one chain (# 4), 2-fold correlation was observed.

Table 3. Summary of the observed decay chains. In the second column, Ju denotes the experimental period of July, Sp that of September, and No that of November. **a**: full energy release in the PSD, **b**: the energy was measured as sum of PSD and SSD signals.

			$\alpha 1$	^{271}Ds		$\alpha 2$	^{267}Hs		$\alpha 3$	^{263}Sg		$\alpha 4$	^{259}Rf		$\alpha 5$	^{255}No	
#		$E_{\rm proj}$ (MeV)	ΔT (ms)	E_α (MeV)		ΔT (ms)	E_α (MeV)		ΔT (ms)	E_α (MeV)		ΔT (s)	E_α (MeV)		ΔT (s)	E_α (MeV)	
1	Ju	310	7.54	9.91	**b**	40.19	9.83	**a**	2.56	9.16	**b**	13.82	8.78	**a**	411.2	7.80	**b**
2	Ju	313	2.20	10.73	**a**	68.4	9.82	**a**	17.6	8.56	**b**	3.13	8.87	**a**	394.7	8.07	**b**
3	Ju	313	46.0	10.44	**a**	1158.6	9.73	**a**	5998.9	9.31	**a**						
4	Ju	313	87.1	10.33	**a**												
5	Sp	313	4.63	10.73	**b**	172.3	9.82	**b**	675.0	9.13	**a**	3.62	8.89	**a**	0.82	8.06	**a**
6	Sp	316	238.7	10.71	**a**	65.96	9.86	**b**	48.65	9.09	**b**	2.71	8.76	**b**	58.4	7.73	**a**
7	Sp	316	1.74	10.47	**b**	159.4	9.97	**b**	718.7	9.04	**a**	0.43	8.87	**b**	241.5	7.81	**a**
8	Sp	316	1.36	10.48	**b**	11.72	9.82	**a**	404.0	9.15	**b**	1.16	8.88	**a**	167.2	7.81	**b**
9	Sp	316	1.31	10.51	**b**	58.96	9.83	**b**	(959.0	8.83	**a**)	(2.14	8.42	**a**)			
10	Sp	316	0.057	10.73	**a**	147.4	9.83	**a**	1322.5	9.19	**b**	9.14	8.90	**a**			
11	Sp	316	6.59	10.63	**a**	18.00	9.68	**b**	430.0	9.23	**a**	0.63	8.94	**b**	286.9	8.05	**a**
12	Sp	316	3.80	10.65	**b**	39.38	9.89	**a**	650.3	9.30	**b**	0.41	8.86	**a**			
13	No	316	1.69	10.70	**a**	101.66	9.90	**b**	385.9	9.23	**a**						
14	No	316	0.92	10.69	**a**	46.53	9.91	**a**	1751.0	9.30	**b**	3.44	5.94	**b**			

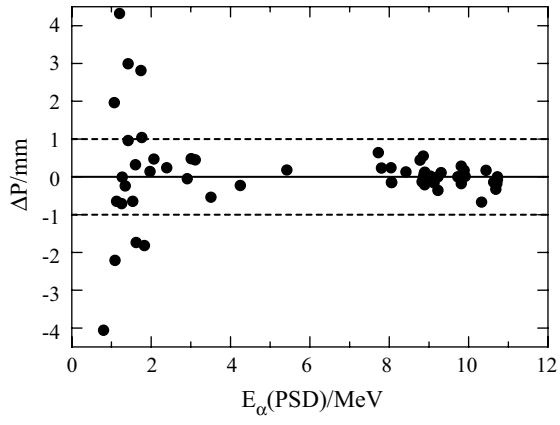

Fig. 3. Position differences between ^{271}Ds implantation and sequential alpha-decays.

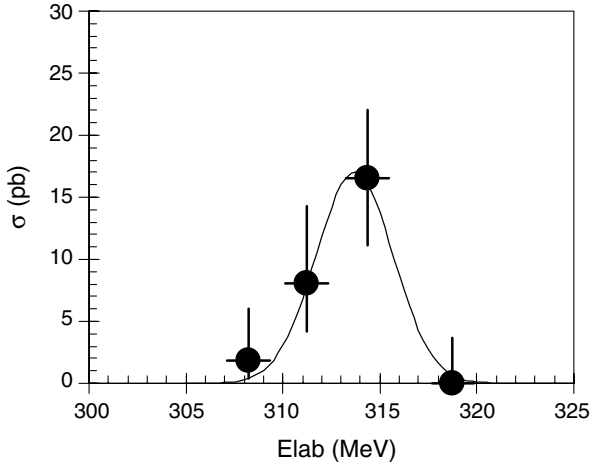

Fig. 4. Excitation function of the production of ^{271}Ds. The horizontal axis indicates the incident energy in the laboratory frame. The errors in the cross-sections are only statistical ones (68% confidence level). The error bars in energies correspond to the energy loss in the targets. Systematic errors are not taken into account.

The position differences between evaporation residues and corresponding alpha-decays are shown in fig. 3. The position resolution has an energy dependence as shown in the figure. Position resolution was better than ±0.9 mm for an energy deposit greater than 2 MeV.

The probability of accidental coincidences was estimated using the counting rate of the decay signal (1 /s) and typical position resolution (1 mm) of the PSD for ER-αn (n = 1–5) correlations, where the decay signal denotes the signal from the PSD detected in anticoincidence to timing counters. The longest correlation time in each n-th correlation was taken for the calculation. No energy selection for the counting rate was made to estimate the maximum probability of accidental coincidence. The results are: 2.5×10^4 for ER-$\alpha 1$, 1.2×10^{-3} for ER-$\alpha 2$, 6.2×10^{-3} for ER-$\alpha 3$, 6.7×10^{-2} for ER-$\alpha 4$, and 0.41 for ER-$\alpha 5$. By multiplying these numbers we get a maximum probability of accidental coincidence for 6-fold correlations of 5.2×10^{-11}, for 5-fold correlations of 1.3×10^{-10}, for 4-fold correlations of 1.9×10^{-9}, and for 2-fold correlation of 2.5×10^{-4}. Because of these estimates of the probability of accidental coincidences, all fourteen correlations were considered to be true correlations. Assignments were based on the comparison of decay energies and decay times of the present data to those reported in refs. [7–9].

In the present experimental setup, the energy threshold of the PSD was set at 1 MeV. Therefore, decaying alphas escaping in the right backward direction were detected neither by PSD nor by SSD. For example, in the # 9 chain, decay times and energies of $\alpha 3$ and $\alpha 4$ (shown in the parentheses in table 3) were put in the column

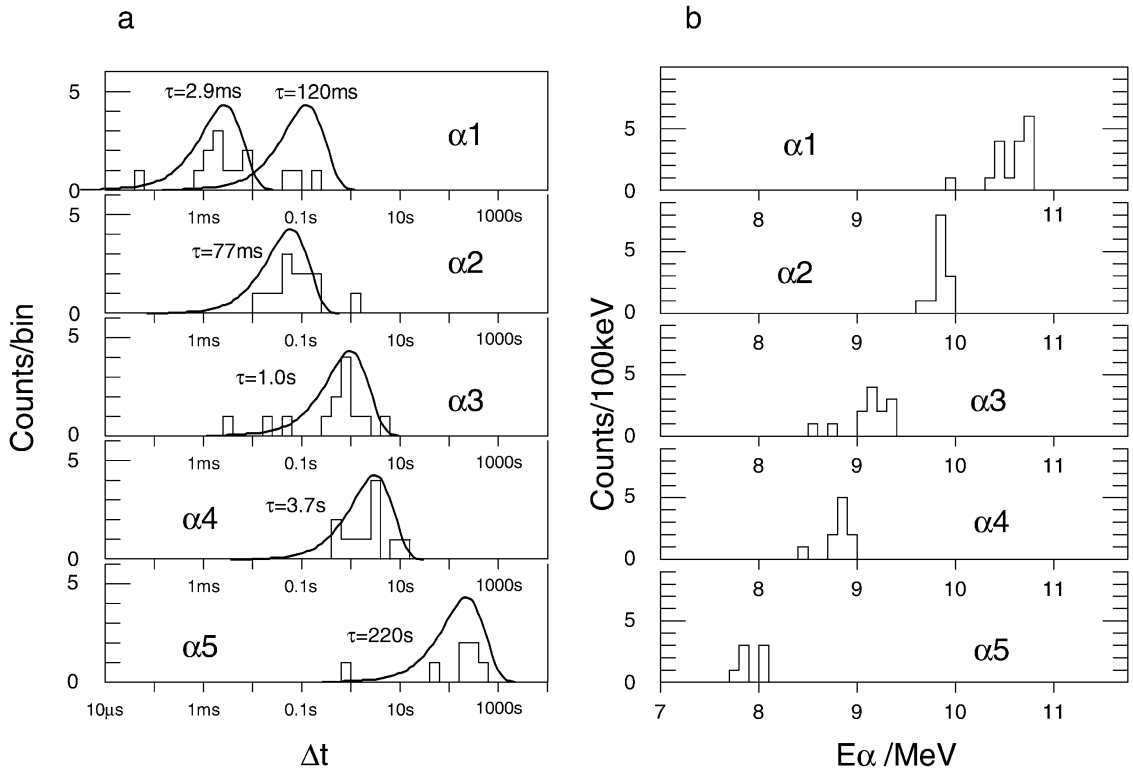

Fig. 5. a: decay time distributions in logarithmic scale. Δt denotes either Δt(ER-α_1) or $\Delta t(\alpha_n$-$\alpha_{n+i})$. The histograms are separated by decay generations $\alpha 1$, $\alpha 2$, $\alpha 3$, $\alpha 4$, and $\alpha 5$. The curves in the figure are decay curves with mean lives (τ) indicated in the figure. Mean lives were obtained in the present work. b: decay energy spectra for each decay generations.

of ^{263}Sg and ^{259}Rf. Although there was no signal registered between the $\alpha 2$ and $\alpha 3$ signals, the possibility that these decays were those of ^{259}Rf and ^{255}No could not be excluded because of considering the decay times and energies. In the # 4 chain, no decay chain was registered following the $\alpha 1$. Although the possibility of three following α-decays emitted into the solid angle of 15% of 4π, which was not covered by the SSD, was 0.3% (0.15^3), we assigned the event also to one originated from ^{271}Ds because of low-background condition.

4 Discussion

4.1 Excitation function

The largest cross-section was obtained at 314 MeV in the laboratory frame corresponding to 240 MeV in the center-of-mass frame, according to a primary-beam energy of 316 MeV. The measured cross-sections are plotted in fig. 4. The curve in the figure is a Gaussian fit by least-square method. The peak position of the curve is 313.8 MeV, and the full width at half-maximum (FWHM) is 4.7 MeV.

In ref. [7] the excitation function was measured at three energies. The maximum cross-section was observed at a primary-beam energy of 313 MeV. With respect to the rather big statistical error, the energy spread of the beam due to energy loss in the target, the accuracy of the estimation of the cross-section maximum, and a possible systematic error of the absolute energies in experiments performed at different accelerators, the difference of our result to that of ref. [7] is not regarded as significant. The energy losses in the target were 2.4 MeV in RIKEN experiment while that at the GSI experiment was 5 MeV.

4.2 Decays of ^{271}Ds

Distributions of decay times and decay energies are presented in fig. 5. The distributions are separated by generations of the decay indicated by $\alpha 1$ to $\alpha 5$.

Figure 5a shows the decay time distribution. The decay times (horizontal axis) are taken in logarithmic scale. A single exponential decay curve is expressed by a universal curve in the figure as proposed in ref. [16]. Curves shown in the figure are such decay curves. The corresponding mean lives are also indicated in the figure.

Figure 5b shows the energy distributions. The measured decay energies of group $\alpha 1$ range from 9.9 to 10.8 MeV. The energy centers of the peak in the spectra were deduced to be 10.45 MeV and 10.73 MeV. The decay energy of ^{271}Ds reported by the GSI group [7,9] was 10.73 MeV. The value agrees well with the higher one of the present result.

Measured decay times of group $\alpha 1$, which were the time difference between the moment of implantation of the nuclei and the first α emissions, are listed in table 3. They could be divided into two groups, one of decay times

shorter than 10 ms (11 events), and another of decay times longer than 10 ms (3 events). The mean life of the first group was calculated to be $2.9^{+1.3}_{-0.7}$ ms and that of the second was 124^{+169}_{-45} ms with errors of 1σ (68%) confidence level. In the top spectrum in fig. 5a, two curves corresponding to decay curves with two mean lives are shown. The theoretical curves well reproduce the shape of the experimental time distributions.

The mean lifetimes of ^{271}Ds reported by the GSI group [7,9] were $1.8^{+0.8}_{-0.4}$ ms (11 events) and 65^{+120}_{-26} ms (2 events), respectively. The values agree for the short lifetime as well as for the long half-life with our results within the error bars (1σ confidence interval). Number ratios of short and long decay time groups, 11/3 by RIKEN group and 11/2 by GSI group, also agree well.

Based on the comparison of the experimental results of the present study and those reported by the GSI group mentioned above, the production of the isotope ^{271}Ds was confirmed. Furthermore, it was proven that the isotope ^{271}Ds has at least two states with different mean lives. We combined the results to get improved values of lifetimes due to better counting statistics. The averaged mean life of the shorter component is $2.35^{+0.64}_{-0.41}$ ms and that of the longer component is 100^{+81}_{-31} ms. The values correspond to half-lives ($T_{1/2}$) of $1.63^{+0.44}_{-0.29}$ ms, and 69^{+56}_{-21} ms, respectively.

4.3 Decay of ^{267}Hs

Thirteen decays detected as second-generation decays ($\alpha 2$) were assigned to be decays of ^{267}Hs. The average energy of $\alpha 2$ was 9.85 MeV. One event (# 3) had a considerably longer decay time than the others. The decay time was 1159 ms while those of the all others (12 events) were less than 200 ms. The mean life of the twelve events was 77^{+31}_{-17} ms. The second frame from top in fig. 5a shows the decay time distribution of the $\alpha 2$ group. The curve in the figure is the decay curve with the obtained mean life (77 ms). We could see from the figure that an event with longer decay time does not belong to the decay group of shorter decay time. The mean life of the isotope ^{267}Hs is reported by Hofmann *et al.* to be 72^{+28}_{-16} ms. It agreed very well with the present value. The measured decay energies of the $\alpha 2$ are listed in table 3 also agree well with the values reported in the refs. [7–9]. Because the isotope ^{267}Hs was previously identified only as decay product of ^{271}Ds, the existence of the isotope is also confirmed by the present work. The mean life deduced by combining the two results is 75^{+19}_{-12} ms. The value corresponds to $T_{1/2} = 52^{+13}_{-8}$ ms.

The observed longer decay time 1159 ms in the # 3 decay chain may be an indication for an isomeric state in ^{267}Hs. A possibility that the state of 52 ms half-life decays with decay time longer than 1159 ms is 2.2×10^{-5}. Therefore we assign it to the decay of an isomeric state $^{267\mathrm{m}}$Hs, that was not observed before. The corresponding half-life of this state is $0.80^{+3.8}_{-0.37}$ s.

4.4 Decay of the isomeric states

Among the first decays of ^{271}Ds, decays of # 3 # 4 and # 6 were assigned to the long decay time group.

In the # 4 chain no following decays were measured. The measured $\alpha 1$ energy was 10.33 MeV.

In the # 6 chain sequential decays after $\alpha 1$ showed no significant difference between other (#1, #2, #5, #7–#14) decays in decay times and energies. The decay energy of #6 was 10.71 MeV. GSI data [9] exhibited two chains starting from longer decay time in the first decays ($\alpha 1$) and showed also no significant difference in the following decays.

On the other hand, in the # 3 decay chain, the second decay, $\alpha 2$, may be assigned to the decay of an isomeric state in ^{267}Hs as discussed in the previous section. The decay energy of the event was 10.44 MeV. Furthermore, the third decay, $\alpha 3$, of this chain also had the longest decay time (5999 ms) of all $\alpha 3$ decays. Although the difference between the longest one and the mean decay time of the $\alpha 3$'s was less significant than the case of second decay ($\alpha 2$), it may be an indication of the isomeric decay of ^{263}Sg. Therefore, the decay of $\alpha 1$, $\alpha 2$, and $\alpha 3$ in the # 3 chain showed the sequential decays of $^{271\mathrm{m}}$Ds $\rightarrow$ $^{267\mathrm{m}}$Hs, and possibly followed by decays of $^{263\mathrm{m}}$Sg.

To understand the decay property of ^{271}Ds observed, the following explanation is possible. An isomeric state exists in ^{271}Ds whose lifetime is much longer than that of the ground state. The isomeric state $^{271\mathrm{m}}$Ds decays by internal transition to the ground state and then decays by alpha emission to the ground state of ^{267}Hs. At the same time, the state $^{271\mathrm{m}}$Ds has another decay mode decaying by alpha to the possible isomeric state $^{267\mathrm{m}}$Hs.

5 Summary

The production and decay of ^{271}Ds were studied through ^{208}Pb + ^{64}Ni $\rightarrow$ ^{271}110 + n reaction using GARIS at RIKEN. In total fourteen decay chains originating from ^{271}Ds were observed. The excitation function of the production cross-section was measured. The energy corresponding to the maximum cross-section was determined to be 239.4 ± 0.6 MeV in the center-of-mass frame. The maximum cross-section value is $16.5^{+7.3}_{-5.5}$ pb. The experimental results confirmed the production and decay properties of ^{271}110 reported by the GSI group. The improved value of the half-life of the ground state of ^{271}Ds is $1.63^{+0.44}_{-0.29}$ ms. The presence of an isomeric state in ^{271}Ds was clearly confirmed and the improved half-life value is 69^{+56}_{-21} ms. The existence and the decay properties of ^{267}Hs were also confirmed. The improved value of the half-life is 52^{+13}_{-8} ms. Evidence for the presence of an isomeric state in ^{267}Hs populated by alpha-decay of $^{271\mathrm{m}}$110 was firstly presented. The measured half-life of this state is $0.80^{+3.8}_{-0.37}$ s.

The authors would like to thank greatly Professors Y. Yano and M. Ishihara for their continuous support, encouragement, and useful suggestions. We would like to thank also Dr M. Kase for

all his support and arrangement about the beam time. Many thanks are due to all accelerator staff members for their excellent operation for a long period of time. The authors would like to thank Professor T. Chihara and Dr N. Suzuki for synthesizing material nickelocene for ion-source. The authors would like to thank Professor J. Peter for his useful suggestions, discussions and comments.

References

1. S. Hofmann, F.P. Heßberger, D. Ackermann, G. Münzenberg, S. Antalic, P. Cagarda, B. Kindler, J. Kojouharova, M. Leino, B. Lommel, R. Mann, A.G. Popeko, S. Reshitko, S. Śaro, J. Uusitalo, A.V. Yeremin, Eur. Phys. J. A **14**, 147 (2002).
2. O. Kamigaito, M. Kase, E. Ikezawa, M. Fujimaki, S. Kohara, N. Fukunishi, N. Sakamoto, M. Hemmi, Y. Miyazawa, Y. Chiba, T. Chiba, A. Goto, Y. Yano, *Proceedings of the 26th Linear Accelerator Meeting in Japan, Tsukuba (2001)*, p. 43.
3. T. Nakagawa, J. Ärje, Y. Miyazawa, M. Hemmi, T. Chiba, N. Inabe, M. Kase, T. Kageyama, O. Kamigaito, A. Goto, M.G. Niimura, Y. Yano, Nucl. Instrum. Methods A **396**, 9 (1997).
4. O. Kamigaito, A. Goto, Y. Miyazawa, T. Chiba, M. Hemmi, M. Kase, S. Kohara, Y. Batygin, E. Ikezawa, T. Nakagawa, Y. Yano, Rev. Sci. Instrum. **70**, 4523 (1999).
5. M. Odera, Y. Chiba, T. Tonuma, M. Hemmi, Y. Miyazawa, T. Inoue, T. Kambara, M. Kase, T. Kubo, F. Yoshida, Nucl. Instrum. Methods A **227**, 187 (1984).
6. K. Morita *et al.*, to be published in Nucl. Instrum. Methods.
7. S. Hofmann, Rep. Prog. Phys. **61**, 639 (1998).
8. S. Hofmann, V. Ninov, F.P. Heßberger, P. Armbruster, H. Folger, G. Münzenberg, H.J. Schött, A.G. Popeko, A.V. Yeremin, A.N. Andreyev, S. Śaro, R. Janik, M. Leino, Z. Phys. A **350**, 281 (1995).
9. S. Hofmann, J. Nucl. Radiochem. Sci. **4**, R1 (2003).
10. S. Hofmann, V. Ninov, F.P. Heßberger, P. Armbruster, H. Folger, G. Münzenberg, H.J. Schött, A.G. Popeko, A.V. Yeremin, A.N. Andreyev, S. Śaro, R. Janik, M. Leino, Z. Phys. A **350**, 277 (1995).
11. S. Hofmann, F.P. Heßberger, D. Ackermann, S. Antalic, P. Cagarda, S. Ćwiok, B. Kindler, J. Kojouharova, B. Lommel, R. Mann, G. Münzenberg, A.G. Popeko, S. Śaro, H.J. Schött, A.V. Yeremin, Eur. Phys. J. A **10**, 5 (2001).
12. Yu.A. Lazarev, Yu.V. Lobanov, Yu.Ts. Oganessian, V.K. Utyonkov, F.Sh. Abdullin, A.N. Polyakov, J. Rigol, I.V. Shirokovsky, Yu.S. Tsyganov, S. Iliev, V.G. Subbotin, A.M. Sukhov, G.V. Buklanov, B.N. Gikal, V.B. Kutner, A.N. Mezentsev, K. Subotic, Rhys. Rev. C **54**, 620 (1996).
13. A. Ghiorso, D. Lee, L.P. Somerville, W. Loveland, J.M. Nitschke, W. Ghiorso, G.T. Seaborg, P. Wilmarth , R. Leres, A. Wydler, M. Nurmia, K. Gregorich, R. Gaylord, T. Hamilton, N.J. Hannink, D.C. Hoffman, C. Jarzynski, C. Kacher, B. Kadkhodayan, S. Kreek, M. Lane, A. Lyon, M.A. McMahan, M. Neu, T. Sikkeland, W.J. Swiatecki, A. Türler, J.T. Walton, S. Yashita, Nucl. Phys. A **583**, 861c (1995).
14. T.N. Ginter, K.E. Gregorich, W. Loveland, D.M. Lee, U.W. Kirbach, R. Sudowe, C.M. Folden III, J.B. Patin, N. Seward, P.A. Wilk, P.M. Zielinski, K. Aleklett, R. Eichler, H. Nitsche, D.C. Hoffman, Phys. Rev. C **67**, 064609 (2003).
15. L.C. Northcliffe, R.F. Schilling, Nucl. Data Tables, A **7**, 233 (1970).
16. K.-H. Schmidt, Eur. Phys. J. A **8**, 141 (2000).